

# Dynamics of Paired-Solitons in Quantum Electron Plasmas

Woo-Pyo Hong<sup>a</sup> and Young-Dae Jung<sup>b</sup>

<sup>a</sup> Department of Electronics Engineering, Catholic University of Daegu, Hayang, 712-702, South Korea

<sup>b</sup> Department of Applied Physics, Hanyang University, Ansan, Kyunggi-Do 426-791, South Korea

Reprint requests to W.-P. H.; E-mail: [wphong@cu.ac.kr](mailto:wphong@cu.ac.kr)

Z. Naturforsch. **66a**, 769–773 (2011) / DOI: 10.5560/ZNA.2011-0050

Received April 31, 2011 / revised August 7, 2011

We show the existence of new localized nonlinear structures for the electrostatic potential and the electron density in the form of bright and W-shaped solitons in quantum electron plasmas, respectively, which is modelled by the coupled nonlinear Schrödinger–Poisson equations. The robustness and the conservation of the energy of the solitons are demonstrated by numerical simulations. The sensitivity of the coupling constant on the stability of the paired solitons in the quantum electron plasmas are investigated.

**Key words:** Quantum Plasmas; Schrödinger–Poisson System; Numerical Solutions; Paired Solitons; Dynamical Stability.

**PACS numbers:** 05.45.Yv; 42.65.Tg; 42.81.Dp

Quantum mechanical effects in dense plasmas become increasingly important when the de Broglie length of the charge carriers is comparable to the dimension of the plasma system. Quantum hydrodynamic (QHD) models for charged particle systems and collective interactions have been proposed for describing the behaviours of dense quantum plasmas [1–5]. Ubiquitous presences of quantum plasmas in micro-mechanical systems and ultra-small electronic devices, in laser and microplasmas [6], in dense astrophysical environments [7], as well as in next generation intense laser-solid density plasma interaction experiments and in quantum X-ray free-electron lasers, have brought active research interests (see [8] for review).

Shukla and Eliasson [9] have recently investigated the formation and dynamics of dark and gray envelope solitons and two-dimensional vortices in quantum electron plasmas with fixed ion background, based on a nonlinear Schrödinger–Poisson (SP) system of equations [1–5, 8], in the form of

$$i \frac{\partial \Psi}{\partial t} + A \nabla^2 \Psi + \phi \Psi - |\Psi|^{4/D} \Psi = 0, \quad (1)$$

$$\nabla^2 \phi = |\Psi|^2 - 1, \quad (2)$$

where the wave function  $\Psi$  is normalized by the equilibrium electron density  $\sqrt{n_0}$ , the electrostatic

potential  $\phi$  by  $T_F/e$ , the time  $t$  by  $\hbar/T_F$ , and the space coordinate  $\mathbf{r}$  by the Debye length  $\lambda_D$ , where  $\lambda_D = (\epsilon_0 T_F / n_0 e^2)^{1/2}$  [4, 8]. In here,  $T_F \sim \hbar^2 n_0^{2/3} / m_e$  is the Fermi temperature (neglecting relevant dimensionless constant),  $m_e$  is the electron mass,  $e$  is the magnitude of the electron charge,  $\epsilon_0$  is the electric permittivity,  $\hbar$  is the Plank constant divided by  $2\pi$  [8–10]. The quantum coupling constant  $A = \Gamma_Q/2$ , where  $\Gamma_Q = m e^2 / \hbar^2 \epsilon_0 n_0^{1/3}$ , is the most important parameter for the system, which can be both smaller and larger than unity depending on the physical situation under consideration [8]. More recently, we showed that the localized nonlinear structures in the form of domain-wall (DW) solitons can exist in (1)–(2), admitting a set of conserved quantities [11]. Quasi-stationary solutions in the form of DW solitons, which show anti-correlation between the electron density and the electrostatic potential, were tested numerically to check their robustness [11].

In this work, we show the existence of new localized nonlinear structures for the electrostatic potential and the electron density in the form of bright and W-shaped solitons in quantum electron plasmas, in the SP system, respectively. We demonstrate their robustness by numerical simulations, identify the boundary condition and the quantum coupling constant range for such stable paired solitons.

The one-dimensional quasi-stationary form of (1) and (2) for the solution moving with a constant velocity  $v_0$  with the ansatz  $\Psi = W(\xi)\exp(iKx - i\Omega t)$ , where  $W$  is a complex-valued function of the argument  $\xi = x - v_0 t$ ,  $K$  is the wave number, where  $K = v_0/2A$ , and  $\Omega$  is the frequency shift, is written as [9, 10]:

$$\frac{d^2 W}{d\xi^2} + \lambda W + \frac{\phi(\xi)W}{A} - \frac{|W|^4 W}{A} = 0, \quad (3)$$

$$\frac{d^2 \phi}{d\xi^2} = |W|^2 - 1, \quad (4)$$

where  $\lambda = 1/A$  and  $\Omega = 1 + v_0^2/4A$  are obtained from the boundary conditions;  $\phi(\xi) = 0$  and  $|W| = 1$  at  $|\xi| = \infty$ .

To search for possible solutions by a numerical method, we substitute a complex function  $W(\xi) = w_1(\xi) + iw_2(\xi)$ , where  $w_1$  and  $w_2$  are real functions, into (3) and (4) to obtain a set of coupled nonlinear differential equations:

$$\begin{aligned} w_i'' &= -\frac{1}{A} [w_i - \phi w_i + (w_i^2 + w_{3-i}^2)w_{3-i}], \\ \phi'' &= w_1^2 + w_2^2 - 1, \quad i = 1, 2, \end{aligned} \quad (5)$$

where  $w_i'' = d^2 w_i/d\xi^2$  and  $\phi'' = d^2 \phi/d\xi^2$ . These coupled equations can be solved for stationary solutions using a numerical shooting method based on the Newton–Raphson iteration scheme [12] with the boundary conditions, i.e.,  $|W| = \sqrt{w_1^2 + w_2^2} = 1$  and  $\phi(\xi) = 0$  at  $|\xi| = \xi_b$ .

We emphasize that depending on the boundary conditions in searching for a numerical solution, there may exist numerous solutions in the form of oscillatory, periodic, and solitonic solutions because there are six boundary conditions in the sixth-order system in (5). For example, it was shown that the paired dark and gray solitons [9] exist for the case that the phase shift between the two boundaries is  $180^\circ$ , meaning that  $W$  was set to  $+1$  on the left boundary and to  $-1$  on the right boundary, i.e.,  $w_1 = 1, w_2 = 0$  on the left and  $w_1 = 0, w_2 = 1$  on the right boundaries. For the case of  $w_1 = w_2 = 1/\sqrt{2}$  at both boundaries, it was demonstrated that the SP system also permits DW solitons at a stronger coupling constant region than that of the dark or gray soliton [11].

Figures 1a–b present numerical solutions by plotting the profiles of the electric potential  $\phi(\xi)$  and the electron density  $|\Psi(\xi)|^2$ , respectively, for three

values of  $A$ , under new boundary conditions, i.e.,  $w_1 = 1, w_2 = 0$  imposed at both the left and the right boundary points with  $|\xi_b| = 30$ . The solutions presented in these figures are different from the paired dark and gray solitons [9] and the DW solitons [11] in the sense that the electrostatic potential has a flat-top profile and the electron density shows a W-shaped distribution. The electron density distribution is similar to that of the gray-soliton in [9] in the sense that it has a localized ‘shoulder’ on both sides of the density. However, it is interesting to note that the electron density has double W-shaped double density depletions. It is clearly shown that each W-shaped electron density profile is anti-correlated to the electrostatic potential  $\phi$  which has a flat top distribution. We also find in Figures 1a–b that the width of the electron density broaden as  $A$  increases, while both the height and the flat-top area (or width) of the electrical potential increase with increasing coupling constant.

We solve (1)–(2) utilizing the split-step Fourier method applying the periodic boundary conditions [13, 14] using the stationary solutions in Figures 1a–c as the initial profiles. Figures 2a–c present the time evo-

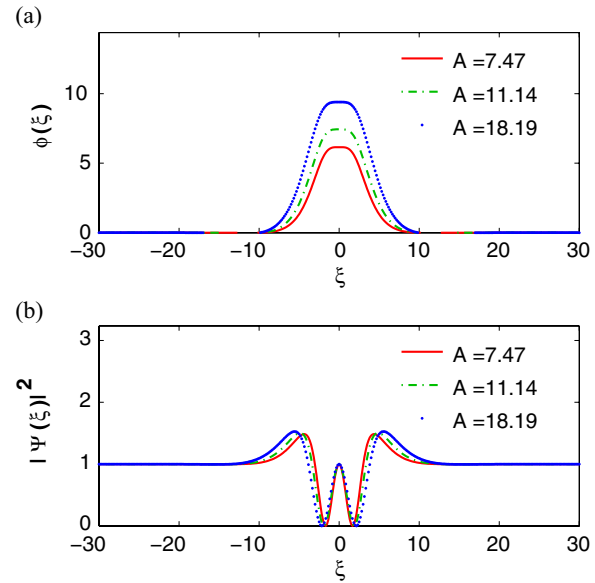


Fig. 1 (colour online). (a) Electrostatic potential  $\phi$ . (b) Electron density  $|\Psi|^2$ . The W-shaped electron density profile is anti-correlated to the electrostatic potential which has a flat top distribution. The width of the electron density is broaden as  $A$  increases, while both the height and the flat-top area of the electrical potential increase with increasing coupling constant.

lutions of the electron density  $|\Psi|^2$  and the electrostatic potential  $\phi$  for the case of zero velocity, i.e.,  $K = v_0/2 = 0$ , with increasing  $A$ . We find that the stability and robustness of the W-shaped solitons and the electric potentials in the form of bright solitons are well maintained up to  $t = 20$ . However, for the cases of  $A = 7.47$  and  $A = 11.14$ , the electrostatic potentials go through breathing at early stage of the evolution before entering into stable propagation after  $t \approx 10$ . On the other hand, both electron densities show stable propagation with minor fluctuations in the W-shaped region. However, for the case of  $A = 18.19$ , the initial potential is quickly stabilized at  $t \approx 5$ , while the electron density shows a stable propagation. This indicates that the only system parameter  $A$  plays a central role in stabiliz-

ing both the electric potential and the electron density during their propagations. The nonlinear Schrödinger–Poisson system conserves the number of electrons as well as their momentum and energy [8–10]. In Figure 2d we show the time development of the total energy of the system [11], defined as

$$\varepsilon(t) = \int \left[ -\Psi(x,t)^* A \partial_x^2 \Psi(x,t) + \frac{1}{2} |\partial_x \phi(x,t)|^2 + \frac{1}{3} |\Psi(x,t)|^6 \right] dx, \quad (6)$$

in order to check the dynamical stability of the solitons. We find that the normalized total energy fluctuates are most strongly at  $A = 7.47$  (solid line), while a minor energy deviation is shown at  $A = 18.19$  (dashed line),

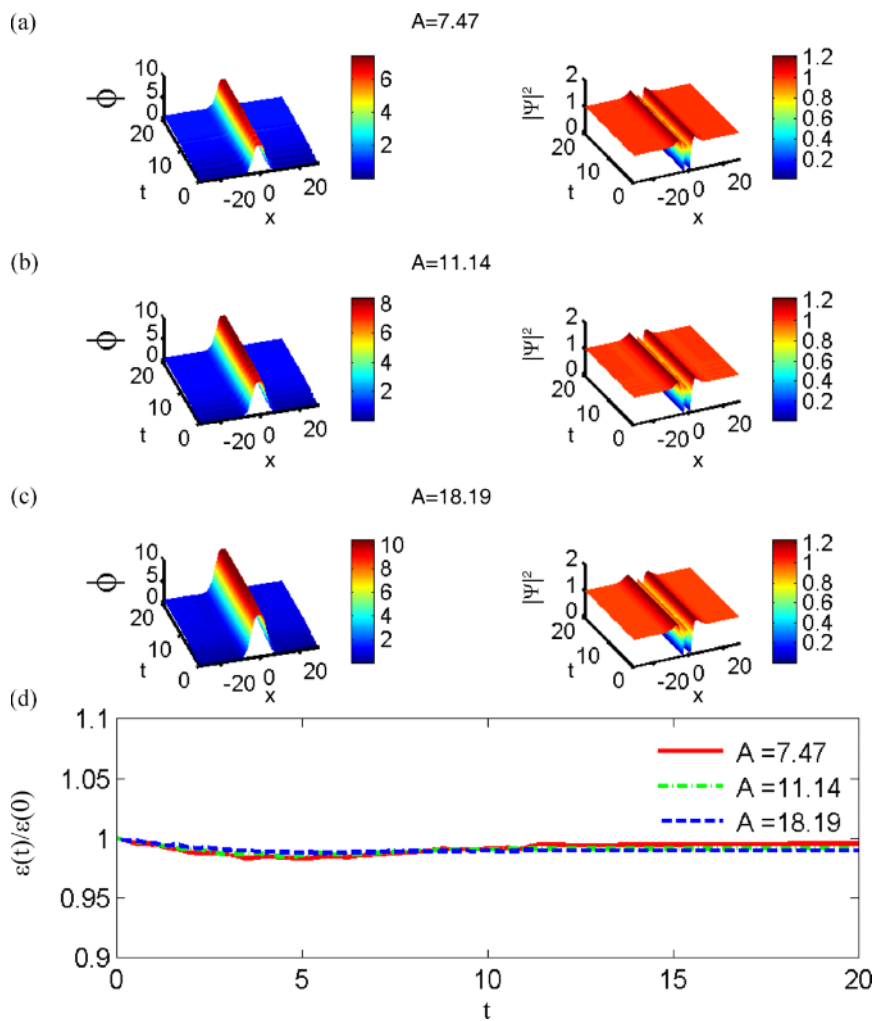


Fig. 2 (colour online). Time evolutions of the electrostatic potential  $\phi$  and the electron density  $|\Psi|^2$  for (a)  $A = 7.47$ , (b)  $A = 11.14$ , and (c)  $A = 18.19$ . The stability and robustness of the W-shaped solitons and the electric potentials are well maintained up to  $t = 20$ . (d) The normalized total energy deviation after  $t \approx 10$  indicates instability, however, which is small enough (less than 1%) to classify them as solitons.

in agreement with the results in Figure 2. The energy deviation after  $t \approx 10$  for all values of  $A$  indicates an instability, however, which is small enough (less than 1%) to classify them as solitons.

We further test how the dynamics of the solutions in Figure 1 are influenced by a perturbation of the coupling constant  $A$ . For example, we use the set of solutions in Figure 1a and perturb  $A$  by  $A' = A + \eta$ , where  $\eta = 0.1A = 0.747$ , to plot their propagations in Figure 3. As shown in Figures 3a–b, the electrostatic potential grows rapidly at  $t \approx 10$ , while the W-shaped electron density becomes highly unstable. This is more clearly illustrated in Figure 1c by the huge energy increase at  $t \approx 10$  and  $t \approx 19$ , which indicates a high instability. Even not shown here, we have confirmed that both the stability of electrostatic potential and the electron density is guaranteed as long as the perturbation is below  $|\eta| < 0.5A$ . We also mention that those solitons in Figures 2a–c under random white noises with less

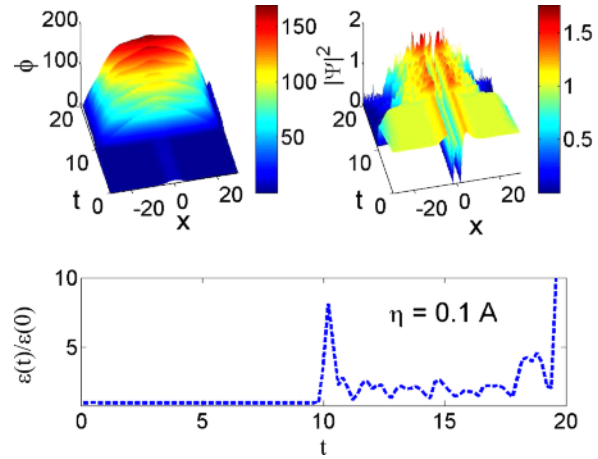


Fig. 3 (colour online). Time evolutions of (a) the electrostatic potential  $\phi$  and (b) the electron density  $|\Psi|^2$ , corresponding to Figure 1a with perturbed coupling constant  $A' = A + \eta$ , where  $\eta = 0.1A = 0.747$ . (c) Huge energy increase at  $t \approx 10$  and  $t \approx 19$  indicate high instability.

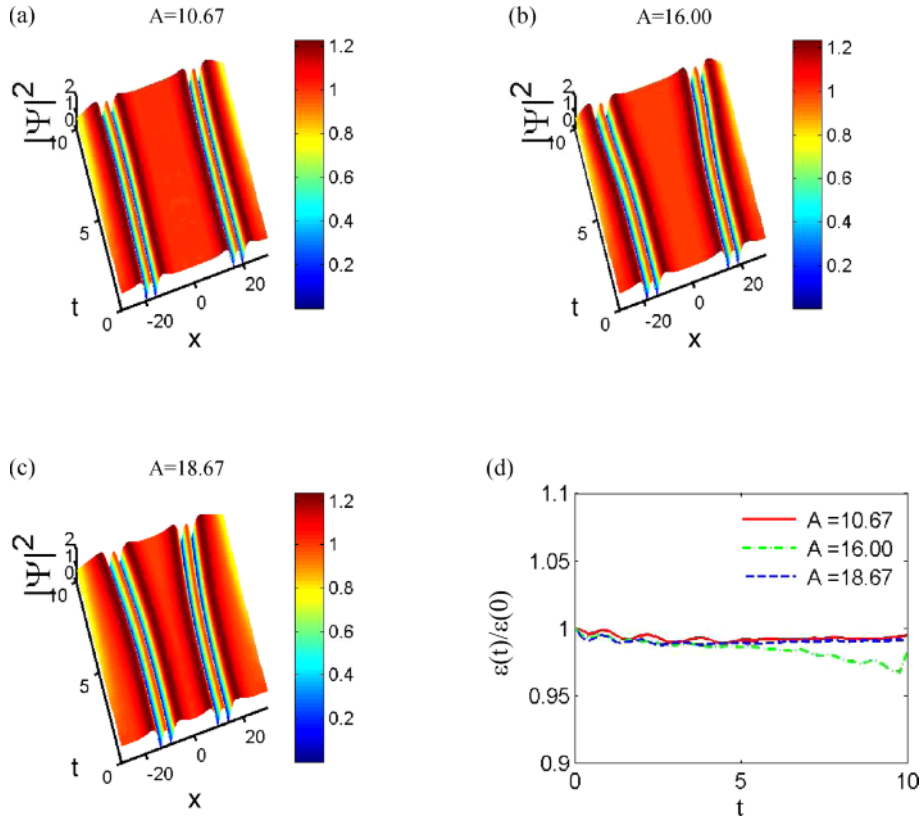


Fig. 4 (colour online). Interaction of two copropagating W-shaped solitons for (a)  $A = 10.67$ , (b)  $A = 16.00$ , and (c)  $A = 18.67$ . The most stable propagation of  $|\Psi|^2$  occurs at  $A = 10.67$ . (d) The energy evolution shows the largest deviation at  $A = 16.00$ .

than 5% of the peak amplitude showed stable propagations.

Finally, we show in Figures 4a–c the interaction of two copropagating electron densities for three different  $A$  values in increasing order. It is clearly demonstrated that a more stable propagation of  $|\Psi|^2$  is obtained at the lowest coupling constant  $A = 10.67$  as shown in Figure 4a. In this case, the shape of the center region of two solitons changes slightly before  $t \approx 5$ , which is indicated by the energy oscillation during its evolution (solid line) in Figure 4d. A stronger interaction at  $A = 16.00$  is shown to occur between the electron densities in Figure 4b. In fact, its energy deviates most strongly, as indicated by the dotted line in Figure 4d. For the case of  $A = 18.67$ , two electron densities are initially attracted most strongly, however, they repel each other after  $t \approx 5$  when the energy approaches to the initial value. From this, we conclude that two electron densities under certain coupling constant regime can be both stable and keep their individual robustness as solitons.

In summary, we have shown the existence of new localized nonlinear structures for the electrostatic potential and the electron density in the form of bright and W-shaped solitons in quantum electron plasmas, respectively, which is modelled by a coupled nonlinear Schrödinger–Poisson equation, admitting a set of

conserved quantities. The quasi-stationary solutions, which show anti-correlation between the W-shaped electron density and the bright-type electrostatic potential, were tested numerically to check their dynamical robustness by using them as initial profiles. It was shown that both the electrostatic potential and the electron density propagate stably by conserving the total energy, as demonstrated in Figure 2. It was found that the stability of both solitons are destroyed when we perturb the coupling constant of the system up to  $\eta = 0.1A$ , as shown in Figure 3. Finally, the copropagating two electron densities were shown to maintain their stability for a distance at the strong coupling constant regime. It was demonstrated that the only parameter  $A$  of the system plays two roles:  $A$  controls the width of the quasi-stationary solution as shown in Figure 1 and acts as the coefficient of the dispersion term in (1). Before closing, we mention that the stability of the numerical solution may shed light on finding some analytical solutions by some symbolic computations [15] or approximate analytical solutions by variational analysis approach [16].

#### Acknowledgement

This work was supported by the funding from Catholic University of Daegu in 2011.

- [1] F. Haas, G. Manfredi, and M. Feix, *Phys. Rev. E* **62**, 2763 (2000).
- [2] G. Manfredi and F. Haas, *Phys. Rev. B* **64**, 075316 (2001).
- [3] D. Anderson, B. Hall, M. Lisak, and M. Marklund, *Phys. Rev. E* **65**, 046417 (2002).
- [4] F. Haas, L. G. Garcia, J. Goedert, and G. Manfredi, *Phys. Plasmas* **10**, 3858 (2003).
- [5] A. V. Andreev, *JETP Lett.* **72**, 238 (2000).
- [6] K. H. Becker, K. H. Schoenbach, and J. G. Eden, *J. Phys. D* **39**, R55 (2006).
- [7] M. Opher, L. O. Silva, D. E. Dauger, V. K. Decyk, and J. M. Dawson, *Phys. Plasmas* **8**, 2454 (2001).
- [8] P. K. Shukla and B. Eliasson, *Phys.-Uspekhi* **53**, 51 (2010).
- [9] P. K. Shukla and B. Eliasson, *Phys. Rev. Lett.* **96**, 245001 (2006).
- [10] D. Shaikh and P. K. Shukla, *Phys. Rev. Lett.* **99**, 125002 (2007).
- [11] W. P. Hong and Y. D. Jung, *Phys. Lett. A* **374**, 4599 (2010).
- [12] Y. H. Ja, *Opt. Quant. Electron.* **15**, 529 (1983).
- [13] J. A. C. Heideman and B. M. Herbst, *SIAM J. Numer. Anal.* **23**, 485 (1986).
- [14] W. P. Hong, *Optics Comm.* **281**, 6112 (2008).
- [15] B. Tian and Y. T. Gao, *Eur. Phys. J. D* **33**, 59 (2005); *Phys. Plasmas* **12**, 054701 (2005); **12**, 070703 (2005); *Phys. Lett. A* **340**, 243 (2005); **340**, 449 (2005); **362**, 283 (2007).
- [16] E. R. Arriola and J. Soler, *J. Stat. Phys.* **103**, 1069 (2001).